Temperature-Dependent Photochemistry of 1,3-Diphenylpropenes. The Di-π-Methane Reaction Revisited

Frederick D. Lewis,*,† Xiaobing Zuo,† Rajdeep S. Kalgutkar,† Jill M. Wagner-Brennan,† Miguel A. Miranda,‡ Enrique Font-Sanchis,‡ and Julia Perez-Prieto§

Contribution from the Department of Chemistry, Northwestern University, Evanston, Illinois 60208-3113, Departmento de Química-Instituto de Tecnologia Quimica UPV-CSIC, Universidad Politécnica de Valencia, Valencia, E-46071 Spain, and Departamento de Química Organica-Instituto de Ciencia Molecular, Facultad de Farmacia, Universidad de Valencia, Burjassot, E-46100 Spain

Received June 4, 2001

Abstract: The temperature-dependent photochemical behavior of 1,3-diphenylpropene and several of its 3-substituted derivatives has been investigated over a wide temperature range. The singlet state is found to decay via two unactivated processes, fluorescence and intersystem crossing, and two activated processes, trans,-cis isomerization and phenyl-vinyl bridging. The latter activated process yields a diradical intermediate which partitions between ground-state reactant and formation of the di-π-methane rearrangement product. Kinetic modeling of temperature-dependent singlet decay times and quantum yields of fluorescence, isomerization, di-π-methane rearrangement, and nonradiative decay provides rate constants and activation parameters for each of the primary and secondary processes. Substituents at the 3-position are found to have little effect on the electronic spectra or unactivated fluorescence and intersystem crossing pathways. However, they do effect the activated primary and secondary processes. Thus, the product ratios are highly temperature dependent.

Introduction

The di-π-methane (Zimmerman) rearrangement is among the most extensively studied unimolecular photochemical reactions.[1] The generalized mechanism proposed by Zimmerman and co-workers for acyclic dienes which react via the singlet state is outlined in Scheme 1. According to this mechanism, the primary photoprocess is vinyl-vinyl bridging leading to the formation of the cyclopropyldicarbinyl diradical **Ia** which proceeds to the 1,3-diradical **Ib**, the precursor of the vinylcylopropane product. It was pointed out by Zimmerman[1a] that **Ia** is not necessarily an energy minimum in singlet di-π-methane rearrangements and that the excited-state potential energy surface could be dependent upon the choice of reactant. The potential energy surface calculated by Bernardi, Robb, and co-workers[2] for the rearrangement of 1,4-pentadiene leads directly from the singlet state to the 1,3-diradical **Ib** via a 1,2-vinyl migration.

Di-π-methane rearrangements are also observed for systems in which one of the π-bonds is part of a phenyl group. The photochemical rearrangement of *trans*-1,3-diphenylpropene (t-**1**) to *trans*-1,2-diphenylcyclopropane (Scheme 2) was originally reported by Griffin et al.[3] and its mechanism was subsequently investigated both by Hixson[4] and by Zimmerman et al.[5] On the basis of these studies, Hixson[4] proposed that a cyclopropyldicarbinyl diradical is most likely an intermediate in this reaction and that its partitioning between product formation and reversion to the ground state might account in part for the low quantum yield for rearrangement of t-**1**. Calculation of the excited-state potential energy surface for a molecule the size of t-**1** remains a formidable challenge despite recent advances in computational methods. However, information about the potential energy surfaces for complex photochemical reactions can also be obtained from a combination of experimental measurements and kinetic modeling, as we have

Scheme 1. Di-π-methane Rearrangement Reaction Mechanisms for 1,4-Pentadiene: (i) Zimmerman Mechanism and (ii) Bernardi and Robb Mechanism

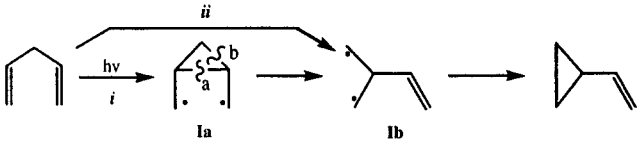

Scheme 2. Photochemical Reactions of 1,3-Diphenylpropenes

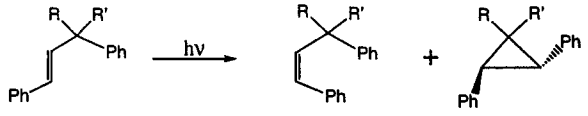

	R	R		
t-1	H	H	c-1 - c-4	p-1 - p-4
t-2	CH_3	H		
t-3	CH_3	CH_3		
t-4	Ph	H		

* To whom correspondence should be addressed. E-mail: lewis@chem.northwestern.edu.

† Northwestern University.

‡ Universidad Politécnica de Valencia.

§ Universidad de Valencia.

(1) For reviews see: (a) Zimmerman, H. E. *Org. Photochem.* **1991**, *11*, 1−36. (b) Zimmerman, H. E.; Armesto, D. *Chem. Rev.* **1996**, *96*, 3065−3112.

(2) Ruguero, M.; Bernardi, F.; Jones, H.; Olivucci, M.; Ragazos, I. N.; Robb, M. A. *J. Am. Chem. Soc.* **1993**, *115*, 2073−2074.

(3) Griffin, G. W.; Covell, J.; Petterson, R. D.; Dodson, R. M.; Klose, G. *J. Am. Chem. Soc.* **1965**, *87*, 1410−1411.

(4) Hixson, S. S. *J. Am. Chem. Soc.* **1976**, *98*, 1271−1273.

(5) Zimmerman, H. E.; Steinmetz, M. G.; Kreil, C. L. *J. Am. Chem. Soc.* **1978**, *100*, 4146−4162.

10.1021/ja0113652 CCC: $20.00
Published on Web 11/09/2001

Table 1. Spectroscopic Parameters for the 1,3-Diphenylpropenes at Room Temperature[a]

	λ_{abs}, nm (A)[b]	λ_{fl}, nm	Φ_f[c]	τ_s, ns[c,d]	$10^{-7}\,k_f$, s^{-1}
t-**1**	254, 284, 293	309	0.28	7.2	3.9
t-**2**	250, 284, 292	308	0.080	1.9	4.2
t-**3**	252, 284, 292	307	0.041	0.63	6.5
t-**4**	254, 284, 294	308	0.044	0.68	6.5

[a] Data for methylcyclohexane solution. [b] Shorter wavelength allowed transition, longer wavelength forbidden transitions. [c] Deoxygenated solutions. [d] Fluorescence decays are single exponentials.

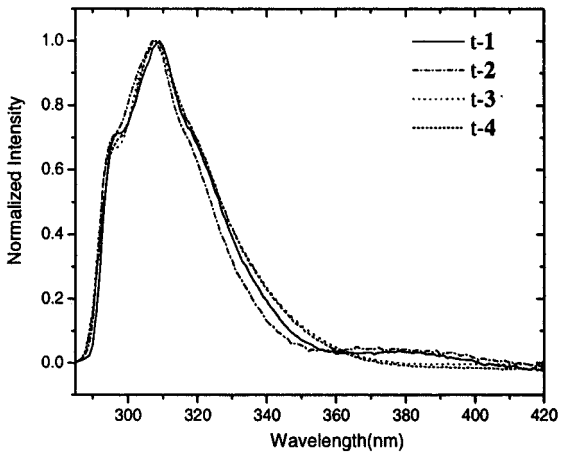

Figure 1. Fluorescence spectra of 1,3-diphenylpropenes t-**1**−t-**4** in methylcyclohexane at room temperature.

recently demonstrated in an investigation of the photochemical behavior of t-**3**.[6]

We report here the results of our collaborative investigation of the potential energy surfaces for the photochemical reactions of t-**1** and its 3-substituted derivatives t-**2**, t-**3**, and t-**4** (Scheme 2). The singlet lifetimes and quantum yields of fluorescence and of formation of the cis isomers c-**1**−c-**4** and the cyclopropanes p-**1**−p-**4** have been determined over a wide temperature range. Kinetic modeling of these data provides conclusive evidence for the formation of the cis isomers via both singlet and triplet pathways and for cyclopropane formation and nonradiative decay via a common intermediate. Modeling further provides activation parameters for both of the activated primary photoprocesses and for the partitioning of this intermediate, as well as for the dependence of these processes upon substituents at the 3-position.

Results

Electronic Spectra. The *trans*-1,3-diphenylpropenes t-**1**−t-**4** were prepared by standard literature procedures and purified to >99% by column chromatography. Their electronic absorption spectra in methylcyclohexane (MC) solution consist of a weak long-wavelength band which displays vibrational structure (two resolved maxima) and a stronger, structureless band at shorter wavelength. The appearance of these bands is similar to that of 1-phenylpropene and is independent of the nature of the 3-substituents. The wavelengths (λ_{abs}) and intensities of the longest wavelength absorption maxima are summarized in Table 1.

The fluorescence spectra of t-**1**−t-**4** are shown in Figure 1 and also resemble that of *trans*-1-phenylpropene.[7] All of the diphenylpropenes display weakly structured room-temperature fluorescence with maxima at 308 ± 1 nm. The very weak emission observed at longer wavelength for t-**3** and t-**4** is artificially amplified by the normalization process. The fluorescence emission maxima (λ_{fl}), quantum yields (Φ_f), and singlet decay times (τ_s) measured at room temperature in MC solution are reported in Table 1. Single-exponential fluorescence decays were obtained in all cases. The values of Φ_f and τ_s are dependent upon the nature of the 3-substituents. The values of τ_s for t-**1** and t-**3** are similar to those previously obtained by Hixson in MC solution (9.7 and 0.65 ns, respectively).[4]

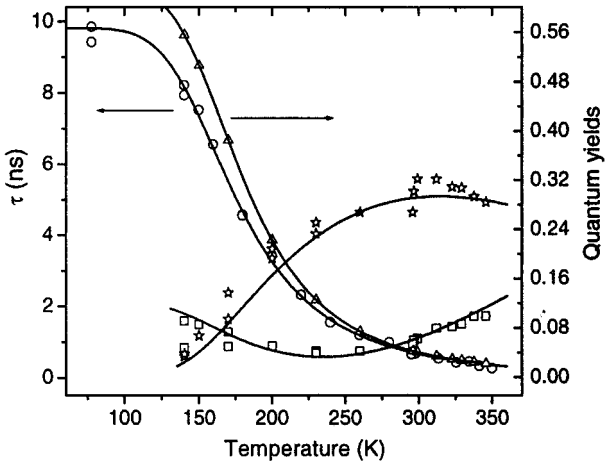

Figure 2. Temperature dependence of the singlet lifetime (○), fluorescence quantum yield (△), cis,trans isomerization quantum yield (□), and di-π-methane rearrangement product formation quantum yield (☆) of 1,3,3-triphenyl-propene (t-**4**) over the temperature range 140−352 K.

Values of Φ_f (140−352 K) and τ_s (77−352 K) have also been determined at a number of temperatures. Fluorescence quantum yields cannot be accurately measured below the glass transition temperature of MC (ca. 140 K) because of volume contraction and light scattering by the occurrence of crystallization upon freezing.[8] The data obtained for t-**4** are shown in Figure 2 and tabular data for all of the diphenylpropenes provided as Supporting Information. The low temperature fluorescence quantum yields have been corrected as described in the Experimental Section. The fluorescence maxima are not strongly temperature dependent, however, the vibrational structure is better resolved at low temperatures. No phosphorescence is observed even at 77 K, as previously reported for 1-phenylpropene.[7]

Photochemical Behavior. The photochemical behavior of t-**1** and t-**3** has been the subject of several previous investigations.[3−5] Direct irradiation yields two primary photoproducts, the cis isomers c-**1** and c-**3** and the 1,2-diphenylcyclopropanes p-**1** and p-**3** (Scheme 2). Analogous products are observed for t-**2** and t-**4**. Triplet sensitized irradiation results exclusively in formation of the cis isomers. Quantum yields for trans,cis isomerization (Φ_{iso}) and di-π-methane rearrangement ($\Phi_{di\pi}$) upon direct irradiation and triplet sensitized trans,cis isomerization (Φ_{sens}) at room temperature in MC solution are summarized in Table 2. The value of $\Phi_{di\pi}$ for t-**1** reported in Table 2 is taken from Hixson[4] and the value determined for t-**3** is the same as that reported by Hixson.[4] The value of Φ_{sens} for t-**3** is similar to that reported by Zimmerman et al.[5] The temperature dependence of Φ_{iso} and $\Phi_{di\pi}$ have also been determined over the range 140−352 K. The data obtained for t-**4** are shown in Figure 2. Tabular data for all of the diphenylpropenes are

(6) Lewis, F. D.; Zuo, X.; Kalgutkar, R. S.; Miranda, M. A.; Font-Sanchis, E.; Perez-Prieto, J. *J. Am. Chem. Soc.* **2000**, *122*, 8571−8572.

(7) Lewis, F. D.; Bassani, D. M.; Caldwell, R. A.; Unett, D. J. *J. Am. Chem. Soc.* **1994**, *116*, 10477−10485.

(8) Liang, A. C.; Willard, J. E. *J. Phys. Chem.* **1968**, *72*, 1018−1023.

Table 2. Quantum Yields for Photoisomerization, Di-π-Methane Rearrangement, and Nonradiative Decay and the Diradical Partition Function at Room Temperature[a]

	Φ_{iso}[b]	Φ_{sens}[c]	$\Phi_{di\pi}$[b]	Φ_{nr}[d]	f[e]
t-**1**	0.30	0.52	0.005[f]	0.12	0.04
t-**2**	0.11	0.47	0.21	0.49	0.30
t-**3**	0.074	0.45	0.42	0.39	0.52
t-**4**	0.059	0.45	0.30	0.54	0.36

[a] Data for methylcyclohexane solution. [b] Direct irradiation of nitrogen-purged solutions. [c] Benzophenone-sensitized irradiation of degassed solutions. [d] Calculated using eq 6. [e] Diradical partition function calculated using eq 12. [f] Data from ref 4.

Scheme 3. Photoisomerization Pathways

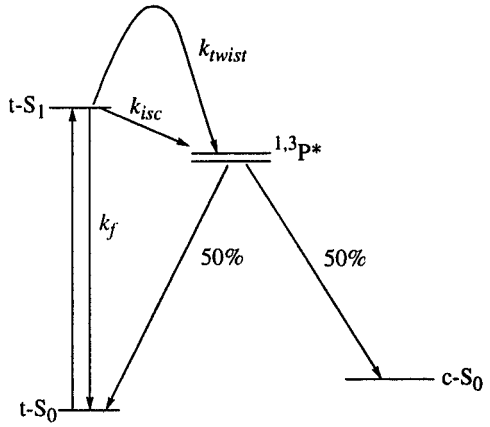

provided as Supporting Information. In the case of t-**1** the values of $\Phi_{di\pi}$ are too low to permit accurate determination below room temperature with our apparatus.

Discussion

Electronic Spectra. The absorption and fluorescence spectra of the diphenylpropenes resemble those of styrene and 1-phenylpropene.[7] The long-wavelength absorption and fluorescence of styrene are assigned to a forbidden ^1L_b transition, thus accounting for the weak absorption and relatively long radiative lifetime. The presence of 3-alkyl or phenyl substituents in t-**2**−t-**4** has little effect on the appearance of the absorption or fluorescence spectra in accord with the SCF−CI calculations of Zimmerman et al.[5] which showed that excitation is localized on the styryl portion of t-**1** in the Franck−Condon excited state.

The fluorescence rate constants for the diphenylpropenes can be calculated from the measured quantum yields and lifetimes ($k_f = \Phi_f\tau_s$). The value reported in Table 1 for t-**1** is similar to that for 1-phenylpropene ($k_f = 3.0 \times 10^7$ s^{-1}).[7] Slightly larger values are observed for the 3-substituted derivatives t-**2**−t-**4**. These observations suggest that the radiative rate may be enhanced by weak interactions of the styrene chromophore with the 3-phenyl substituents, interactions which presumably depend on the ground-state conformation.

Trans,cis Photoisomerization. In their study of t-**3**, Zimmerman et al.[5] determined that the quantum yield for trans,cis isomerization obtained upon direct irradiation was significantly smaller than that obtained upon triplet sensitized irradiation ($\Phi_{iso} = 0.065$ and $\Phi_{sens} = 0.51$). Based on this observation, they proposed that isomerization of t-**3** occurs predominately via intersystem crossing. Our subsequent study of the photoisomerization of *trans*-1-phenylpropene established that isomerization can occur via both an activated singlet state pathway and an unactivated triplet pathway, the latter dominating at or below room temperature and the former dominating at higher temperatures.[7,9] As shown in Scheme 3, both pathways lead to twisted intermediates (^{1}P* or ^{3}P*) which decay to an equal mixture of ground-state trans and cis isomers. We have confirmed that $\Phi_{sens} = 0.50 \pm 0.05$ for t-**1**−t-**4** (Table 2). According to Scheme 3, the total isomerization quantum yield is described by eq 1 and eqs 2 and 3 describe the phenomenological and analytical isomerization rate constants, respectively,

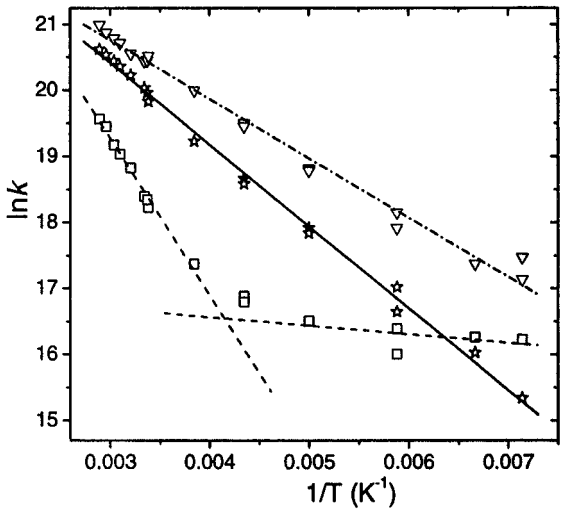

Figure 3. Arrhenius plots of the rate constants of cis,trans isomerization (□), di-π-methane rearrangement (☆), and nonradiative decay (▽) vs temperature for t-**4**.

$$\Phi_{iso} = 0.5k_{twist}\tau_s + 0.5k_{isc}\tau_s \quad (1)$$

$$k_{iso} = \Phi_{iso}\tau_s^{-1} \quad (2)$$

$$k_{iso} = \frac{1}{2}\left[k_{isc} + A_{twist}\exp\left(\frac{-\Delta E_{twist}}{RT}\right)\right] \quad (3)$$

where k_{twist} is the rate constant for singlet state isomerization and k_{isc} is the rate constant for intersystem crossing.

An Arrhenius plot ($\ln(k_{iso})$ vs T^{-1}) of the isomerization data for t-**4** is shown in Figure 3. The nonlinear nature of this plot is similar to that observed previously for the isomerization of 1-phenylpropene and is consistent with the occurrence of both an activated (singlet) and an unactivated (triplet) mechanism for isomerization (Scheme 3). Activation parameters for the singlet state process and the intersystem crossing rate constant can be estimated from this plot. However, more accurate parameters can be obtained from nonlinear fitting of the temperature dependence of k_{iso} according to eq 3 (Figure 4). Values of the intersystem crossing rate constant, k_{isc}, and activation parameters for singlet state twisting obtained from nonlinear fitting of data for all of the diphenylpropenes are reported in Table 3. The values of k_{isc} are similar to the value reported for 1-phenylpropene (4.6×10^7 s^{-1}).[7]

The values of A_{twist} for all of the diphenylpropenes are larger than that for 1-phenylpropene (0.63×10^{12} s^{-1})[7] and are consistent with a singlet state twisting mechanism. Similar values of A_{twist} are obtained for t-**1**−t-**3** whereas a somewhat lower value is found for t-**4**. The values of ΔE_{twist} for the diphenylpropenes are all smaller than that for 1-phenylpropene (8.8 kcal/mol in hexane solution). Values of ΔE_{twist} decrease with the bulk of the 3-substituent (t-**1** > t-**2** > t-**4**); however

(9) For a discussion of the potential energy surfaces for singlet and triplet isomerization of styrene see: Bearpark, M. J.; Olivucci, M.; Wilsey, S.; Bernardi, F.; Robb, M. A. **J. Am. Chem. Soc. 1995**, *117*, 6944−6953.

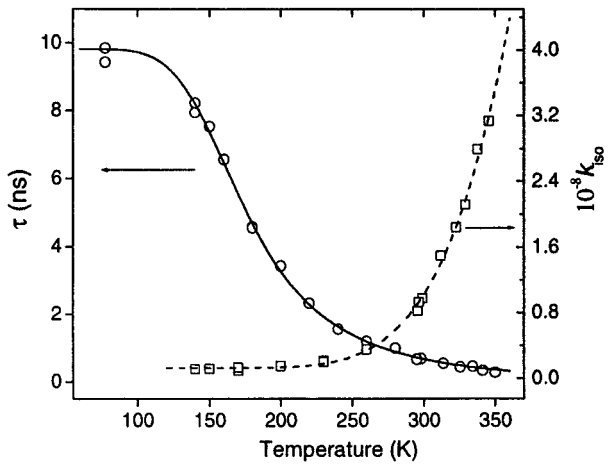

Figure 4. Temperature dependence of the singlet lifetime, τ (○), and rate constant for cis,trans isomerization, k_{iso} (□), for t-**4**.

Table 3. Rate Constants for Intersystem Crossing and Activation Parameters of Singlet State Cis,trans Photoisomerization[a]

	$10^{-7}\ k_{isc}$, s^{-1}	$10^{-13}\ A_{twist}$	ΔE_{twist}, kcal/mol
t-**1**	5.0	1.3	7.6
t-**2**	5.1	0.74	6.6
t-**3**	3.1	1.3	6.6
t-**4**	3.7	0.20	5.6

[a] Calculated by fitting of the k_{iso} data to eq 3 as shown for t-**4** in Figure 4.

no further decrease is observed for the 3,3-disubstituted t-**3**. These changes plausibly reflect the increase in steric energy of the planar singlet vs twisted singlet, which would result in a lower barrier for twisting (Scheme 3).

Di-π-methane Rearrangement. Zimmerman et al.[5] determined that the quantum yield for formation of p-**3** upon direct irradiation is significantly larger than that for triplet sensitized irradiation ($\Phi_{di\pi} = 0.40$ and <0.003, respectively), in accord with a singlet rearrangement mechanism. The rate constant $k_{di\pi}$ can be described by a phenomenological rate expression, eq 4, which is analogous to eq 2.

$$k_{di\pi} = \Phi_{di\pi}\tau_s^{-1} \tag{4}$$

An Arrhenius plot for the temperature dependence of the data for t-**4** is shown in Figure 3. The linear nature of this plot is consistent with an activated singlet state rearrangement mechanism. Activation parameters for the rearrangement process can be estimated from this plot. However, if the intermediate **Ia** (Scheme 1) undergoes return to the ground state in competition with product formation, as suggested by Hixson,[4] the measured value of $\Phi_{di\pi}$ would underestimate the quantum yield for phenyl-vinyl bridging.

Activation parameters for the rate determining step in the di-π-methane rearrangement, k_{pv}, and the intersystem crossing rate constant, k_{isc}, can be obtained from nonlinear fitting of the temperature dependence of the singlet decay time according to eq 5, using the previously determined values of k_f, A_{twist}, and ΔE_{twist} (Tables 1 and 3).

$$\tau_s = \frac{1}{k_f + k_{isc} + A_{pv}\exp\left(\frac{-\Delta E_{pv}}{RT}\right) + A_{twist}\exp\left(\frac{-\Delta E_{twist}}{RT}\right)} \tag{5}$$

This expression is valid for both rate determining phenyl-vinyl bridging (Scheme 1, Zimmerman mechanism) and phenyl-vinyl 1,2-migration (Bernardi-Robb mechanism). A plot of the temperature-dependent lifetime for t-**4** is shown in Figure 4, and the values of A_{pv} and ΔE_{pv} obtained from nonlinear fitting are reported in Table 4, along with the room-temperature values of k_{pv} calculated using these activation parameters.

Table 4. Rate Constants at Room Temperature and Activation Parameters for Phenyl-Vinyl Bridging[a]

	k_{pv}, s^{-1}	$10^{-10}\ A_{pv}$	ΔE_{pv}, kcal/mol
t-**1**	2.1×10^7	0.94	3.6
t-**2**	3.5×10^8	1.2	2.1
t-**3**	1.5×10^9	4.3	2.0
t-**4**	1.2×10^9	4.3	2.1

[a] Calculated by fitting the singlet lifetime data to eq 5, as shown for t-**4** in Figure 4.

Scheme 4. Calculated Ground-State Bond Angle θ for t-**1**−t-**4**

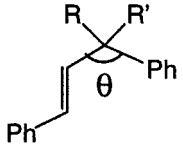

	R	R'	θ(°)
t-1	H	H	116.8
t-2	CH_3	H	113.7
t-3	CH_3	CH_3	113.9

The room-temperature values of k_{pv} increase upon introduction of 3-methyl substituents, following the order t-**1** < t-**2** < t-**3**. Hixson[4] attributed the large increase in the apparent rate constant for the di-π-methane rearrangement of t-**3** vs t-**1** to the *gem*-dialkyl effect. According to the classical Thorpe-Ingold explanation, compression of the internal angle between reactive groups can account for this effect.[10] As shown in Scheme 4, the calculated ground-state dihedral angles for t-**2** and t-**3** are similar and smaller than that for t-**1**. More modern explanations for the *gem*-dialkyl effect attribute rate enhancements to a decrease in population of ground-state unreactive rotamers[11a] or to overall reductions in the enthalpy of reaction resulting from changes in both ground- and transition-state enthalpies.[11b] In most examples of the *gem*-dialkyl effect, a single alkyl substituent causes much smaller rate enhancement than dialkyl substitution.[10,11] However, the rate enhancement observed for t-**2** vs t-**1** is larger than that observed for t-**3** vs t-**2** (Table 4). Furthermore, the values of ΔE_{pv} for the two latter molecules are essentially the same, the increased rate for t-**3** resulting primarily from the increase in A_{pv}. Thus, the rate enhancement observed upon 3-alkylation of the diphenylpropenes is a consequence of complex changes in the entropy and enthalpy of activation.

When compared to activated (singlet) isomerization (Table 3), the rate determining step for the di-π-methane rearrangement has significantly lower preexponentials and activation energies (Table 4). The lower preexponentials are consistent with a decrease in entropy, as would be expected for either phenyl-vinyl bridging or 1,2-phenyl-vinyl migration as the rate-determining step (Scheme 1). As a consequence of the lower activation energies, values of $\Phi_{di\pi} > \Phi_{iso}$ are observed for t-**2**−t-**4** at temperatures between 180 and 350 K (Figure 2). At temperatures < 160 K both activated processes become slower than k_{isc} and k_f. Thus, triplet isomerization and fluorescence become the major excited-state processes. At higher temperatures the ratio $\Phi_{di\pi}/\Phi_{iso}$ decreases as a consequence of the larger A value for singlet isomerization and isomerization is expected

(10) Beesley, R. M.; Ingold, C. K.; Thorpe, J. F. *J. Chem. Soc.* **1915**, 1080−1106.

(11) (a) Lightstone, F. C.; Bruice, T. C. J. *J. Am. Chem. Soc.* **1994**, *116*, 10789−10790. (b) Parrill, A. L.; Dolata, D. P. J. *Tetrahedron Lett.* **1994**, *35*, 7319−7322.

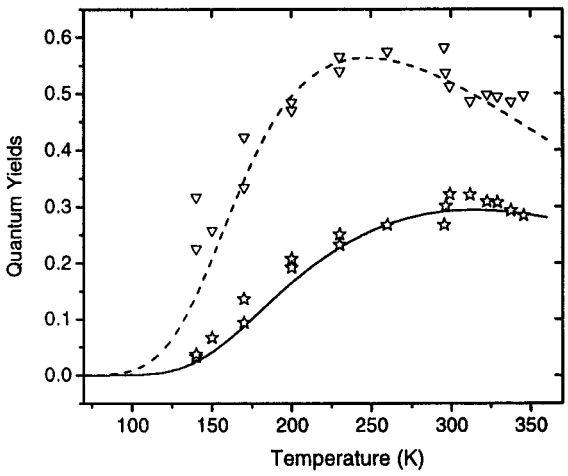

Figure 5. Simultaneous kinetic fitting of the di-π-methane rearrangement product formation quantum yield (☆) and nonradiative decay quantum yield (▽) for t-**4**.

to be the major process at very high temperatures (>440 K). In the case of t-**1**, intersystem crossing and fluorescence are more rapid than either activated process for the entire temperature range.

Nonradiative Decay. Hixson[4] suggested that the much lower quantum yield for rearrangement of t-**1** vs t-**3** (Table 2) might arise in part from reversion of the bridged intermediate **Ia** to the starting olefin in competition with ring-opening to form the diradical **Ib**, the precursor of the cyclopropane product (Scheme 1). A nonradiative decay pathway is necessary to account for the inefficiencies in radiative and product forming reactions. The quantum yield for nonradiative decay, Φ_{nr}, can be calculated using eq 6,

$$\Phi_{nr} = 1 - (\Phi_f + 2\Phi_{iso} + \Phi_{di\pi}) \quad (6)$$

where it assumed that both the singlet and triplet pathways for photoisomerization involve twisted intermediates which decay with equal probability to the trans starting material and its cis isomer (Scheme 3), as is the case for 1-phenylpropene.[7,12] Calculated room-temperature values of Φ_{nr} are reported in Table 2 and are seen to account for a significant fraction of the singlet state decay for t-**2**−t-**4** and a smaller fraction for t-**1**.

The temperature dependence of Φ_{nr} can also be calculated from the temperature-dependent quantum yield data using eq 6. The resulting values for t-**4** are shown in Figure 5 along with the data for $\Phi_{di\pi}$. The values of Φ_{nr} display a maximum at ca. 250 K, decreasing at both higher and lower temperatures. By analogy to eqs 2 and 4, the phenomenological rate constants for nonradiative decay can be described by eq 7.

$$k_{nr} = \Phi_{nr}\tau_s^{-1} \quad (7)$$

An Arrhenius plot of the temperature dependence of k_{nr} for t-**4** (Figure 3) is linear over the entire temperature range 140−352 K and provides activation parameters ($A_{nr} = 1.5 \times 10^{10}$ and $\Delta E_{nr} = 1.8$ kcal/mol) that are similar to those obtained from the k_{pv} data for t-**4** (Table 4). This is consistent with the Zimmerman[1] mechanism (Scheme 1) in which nonradiative decay and the di-π-methane rearrangement occur via a common intermediate **Ia**. However, it is apparently inconsistent with the Bernardi-Robb[2] mechanism since the intermediate **Ib** is unlikely to revert to the starting olefin.

(12) Ni, T.; Caldwell, R. A.; Melton, L. A. *J. Am. Chem. Soc.* **1989**, *111*, 457−464.

Scheme 5. Schematic Potential Energy Surface for Di-π-methane Rearrangement of t-**4**

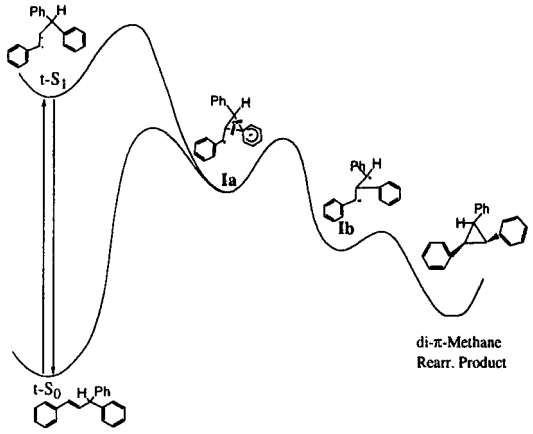

Table 5. Activation Parameters for Nonradiative Decay and Formation of Diradical **Ib**[a]

	$10^{-10} A_{nr}$	ΔE_{nr}, kcal/mol	$10^{-10} A_{Ib}$	ΔE_{Ib}, kcal/mol
t-**2**	0.07	0.28	6.3	3.0
t-**3**	0.69	0.44	8.0	1.9
t-**4**	4.4	0.85	7.0	1.5

[a] Calculated by simultaneous fitting of the quantum yields of di-π-methane product formation and nonradiative decay as shown for t-**4** in Figure 5.

According to the Zimmerman mechanism[1] the intermediate **Ia** proceeds to the rearranged product via a second intermediate **Ib** with a rate constant k_{Ib} in competition with nonradiative decay (Scheme 5). This scheme provides the expressions shown in eqs 8 and 9 for the quantum yields of these two competing processes in terms of the probabilities of forming **Ia** from the singlet state ($P1$) and of forming the rearrangement product from **Ia** ($P2$) (eqs 10 and 11).

$$\Phi_{Ib} = P1 \times P2 \quad (8)$$

$$\Phi_{nr} = P1 \times (1 - P2) \quad (9)$$

$$P1 = \frac{k_{pv}}{k_f + k_{isc} + k_{pv} + k_{twist}} \quad (10)$$

$$P2 = \frac{k_{Ib}}{k_{nr} + k_{Ib}} \quad (11)$$

Assuming that **Ib** is formed irreversibly, $\Phi_{Ib} = \Phi_{di\pi}$. The temperature-dependent quantum yields Φ_{nr} and Φ_{Ib} obtained for t-**4** are shown in Figure 5 along with the results of simultaneous kinetic fitting of these data (Experimental Section) which provides activation parameters for both processes. Activation parameters determined by this procedure for t-**2**−t-**4** are reported in Table 5. In the case of t-**1** the values of $\Phi_{di\pi}$ are too low to permit accurate measurement at low temperatures. Values of ΔE_{Ib} for conversion of **Ia** to **Ib** are seen to decrease for the series t-**2** > t-**3** > t-**4**, whereas values of ΔE_{nr} increase. This result is consistent with the anticipated changes in the cyclopropane exocyclic dihedral angles upon ring opening (Scheme 1). Opening of bond b results in an increase in these bond angles and is thus subject to steric acceleration. In contrast, opening of bond a results in a decrease in these bond angles and thus should be subject to steric deceleration. Alkyl or phenyl substituents can also stabilize the incipient radical center in

intermediate **Ib**, thus favoring path b. This is consistent with the smaller value of $\Delta E_{\mathbf{Ib}}$ for t-**4** than for t-**2**.

As noted previously, Hixson[4] suggested that the larger value of $\Phi_{di\pi}$ for t-**3** than for t-**1** might result from differences in the partitioning of intermediate **Ia** between rearrangement via **Ib** vs starting material (Scheme 5). The efficiency of product formation from **Ia**, *f*, can be quantified using eq 12.

$$f = \Phi_{di\pi}/(\Phi_{di\pi} + \Phi_{nr}) \qquad (12)$$

Values of *f* are summarized along with the room-temperature quantum yield data in Table 2. The values of *f* for t-**1** and t-**3** are similar to those calculated by Hixson. Introduction of a single methyl substituent in t-**2** results in a value of *f* intermediate between those of t-**1** and t-**3**. The phenyl substituent in t-**4** has a value of *f* only slightly larger than that of the methyl substituent in t-**2**. This plausibly reflects an early transition state for bond breaking in **Ia**. The values of *f* are also temperature dependent as a consequence of the different activation parameters for $k_{\mathbf{Ib}}$ and k_{nr}. The former process has the larger activation energy and larger preexponential and thus is favored at higher temperatures, whereas the latter process is favored at lower temperatures (Figure 5).

Concluding Remarks. The results of this investigation provide a complete description of the competing photochemical reactions which occur via the singlet state of several 1,3-diphenylpropenes. These include isomerization via both the singlet and triplet states (Scheme 3) and singlet phenyl-vinyl bridging to yield a diradical intermediate which can either proceed to the di-π-methane product or revert to starting material (Scheme 5). Activation parameters have been determined for both the primary processes (singlet isomerization and phenyl-vinyl bridging) and diradical processes (nonradiative decay and product formation). The results of this analysis are consistent with the stepwise Zimmerman mechanism (Scheme 1, path i) rather than the Bernardi-Robb concerted migration (Scheme 1, path ii). The Bernardi-Robb energy surface for 1,4-pentadiene evidently is not applicable to more complex molecules such as the 1,3-diphenylpropenes. This illustrates the potential hazard of using truncated models to calculate potential energy surfaces for more complex molecules.

Substituents at the 3-position are found to have little effect on either the absorption and fluorescence spectra or the temperature-independent rate constants for fluorescence and intersystem crossing (Tables 1, 3). They do, however, affect the activation parameters for the competing activated singlet state processes, isomerization and phenyl-vinyl bridging (Tables 3, 4). Activation energies for both processes decrease with increasing 3-substitution. Phenyl-vinyl bridging has both a lower activation energy and a lower preexponential than isomerization, and is the dominant reaction pathway for t-**2**−t-**4** at temperatures between 160 and 350 K. At temperatures below 160 K triplet isomerization and fluorescence are the major processes, whereas above 440 K singlet isomerization is expected to be the major pathway.

Substituents at the 3-position also affect the partitioning of the diradical intermediate **Ia** (Scheme 5). Ring opening leading to the product has larger preexponentials and larger activation energies than ring opening to regenerate the ground-state reactant (Table 5), resulting in complex temperature dependence for the quantum yield ratios (Figure 5). Activation energies for the ring opening leading to product decrease with increasing 3-substitution. This could result from either relief of angle strain or stabilization of the diradical **Ib**.

This analysis of the di-π-methane rearrangement serves to further illustrate the power of kinetic modeling of temperature-dependent data sets to elucidate photochemical reaction mechanisms which are too complex for simple kinetic analysis.[13] Applications of these methods to other photochemical processes are in progress in our laboratories.

Experimental Section

Materials. *trans*-1,3-Diphenylpropene (t-**1**) was prepared by heating phenylacetaldehyde and potassium in ethanol using the method of Stoermer et al.[14,15] and was purified by recrystallization at −77 °C from ethanol. *trans*-1,3-Diphenyl-1-butene (t-**2**) was prepared by the method of Higashimura et al.[16] via acetyl perchlorate catalyzed dimerization of styrene and purified by column chromatography. *trans*-1,3-Diphenyl-3-methyl-1-butene (t-**3**) was prepared by a Grignard reaction of neophylmagnesium chloride and benzaldehyde, followed by dehydration of the resulting alcohol catalyzed by *p*-toluenesulfonic acid in benzene, and then finally purified by column chromatography, as described by Zimmerman et al.[5,17] *trans*-1,3,3-Triphenylpropene (t-**4**) was prepared by the method of Ahlberg et al.[18] via the reaction of benzylideneacetophenone and phenylmagnesium bromide, reduction of the resulting ketone with $NaBH_4$, then dehydration of the resulting alcohol. Compounds t-**1**−t-**3** are colorless oils and t-**4** is a colorless crystalline solid mp = 94−95 °C (lit.[18] mp = 98−99 °C). All compounds were found to have greater than 99.9% purity as estimated by GC analysis. The cis olefins c-**1**,[15] c-**2**,[19] and c-**3**[5] were obtained by acetone-sensitized photoisomerization of the corresponding trans-isomers and purified by HPLC. The phenylcyclopropanes p-**2**[20] and p-**3**[5] were obtained from the corresponding *trans*-alkenes by irradiation (medium-pressure mercury lamp, Pyrex filter) in cyclohexane solution. ^{1}H NMR and GC/MS were used to establish the identity and purity of all compounds. Spectral data for the cis isomers and phenylcyclopropanes were identical to those published in the literature. All solvents used for spectroscopy and photolyses were either spectrophotometric or HPLC grade and were used as received.

Experimental Methods. GC analysis was performed on a Hewlett-Packard HP 5890 instrument equipped with a HP1 poly(dimethylsiloxane) capillary column. UV−vis spectra were measured on a Hewlett-Packard 8452A diode array spectrometer with a 1-cm path length quartz cell. Fluorescence spectra were measured on a SPEX Fluoromax spectrometer and are uncorrected. Fluorescence quantum yields for deoxygenated solutions were measured by comparing the integrated area under the fluorescence curve to that for *trans*-1-phenylpropene ($\Phi_f = 0.35$, in hexanes[7]) at equal absorbance at the same excitation wavelength. The fluorescence quantum yields are corrected for the refractive index of the solvent. The estimated error is ±10%. Fluorescence decays were measured on a Photon Technologies International (PTI) LS-1 stroboscopic detection instrument with a gated hydrogen arc lamp using a scatter solution to profile the instrument response function. Nonlinear least-squares fitting of the decay curves was performed with the Levenburg-Marquardt algorithm described by James et al.[21] as implemented by the PTI Timemaster (version 1.2)

(13) For examples see: (a) Saltiel, J. A.; Zhang, Y.; Sears, D. F., Jr. *J. Am. Chem. Soc.* **1997**, *119*, 11202−11210. (b) Catalán, J.; Zimányi, L.; Saltiel, J. *J. Am. Chem. Soc.* **2000**, *122*, 2377−2378. (c) Lewis, F. D.; Li, L.-S.; Kurth, T. L.; Kalgutkar, R. S. *J. Am. Chem. Soc.* **2000**, *122*, 8573−8574.

(14) Stoermer, R.; Their, C.; Laage, E. *Chem. Ber.* **1925**, *B85*, 2607−2615.

(15) Raunio, E. K.; Bonner, W. A. *J. Org. Chem.* **1966**, *31*, 396−399.

(16) (a) Sawamoto M.; Masuda T.; Nishii H.; Higashimura T. *J. Polym. Sci. Polym. Lett. Ed.* **1975**, *13*, 279−282. (b) Higashimura T.; Nishii H. *J. Polym. Sci. Polym. Chem. Ed.* **1977**, *15*, 329−339.

(17) Calcott, W. S.; Tinker, J. M.; Weinmayr, V. *J. Am. Chem. Soc.* **1939**, *61*, 1010−1015.

(18) Ahlberg P.; Janne K.; Lofas S.; Nettelblad F.; Swahn L. *J. Phys. Org. Chem.* **1989**, *2*, 429−447.

(19) Ella, S. W.; Cram, D. J. *J. Am. Chem. Soc.* **1966**, *88*, 5777−5791.

(20) Fox, M. A.; Chen, C. C.; Campbell, K. A. *J. Org. Chem.* **1983**, *48*, 321−326.

(21) James, D. R.; Siemiarczuk, A.; Ware, W. R. *Rev. Sci. Instrum.* **1992**, *63*, 1710−1716.

software. Goodness of fit was determined by judging the χ^2 ($0.8 < \chi^2 < 1.3$ in all cases), the residuals, and the Durbin-Watson parameter (>1.6 in all cases).

Measurements of quantum yields for direct photoisomerization and di-π-methane rearrangement product formation for t-**1**−t-**4** were performed on optically dense deoxygenated solutions ($\sim 10^{-3}$ M) excited at 270 nm. Solutions were deoxygenated by purging with dry N_2 for 20−25 min. The extent of photochemical conversion (<5%) was quantified by GC. Excitation at 270 or 366 nm was achieved with a 200 W high-pressure Hg(Xe) arc lamp and a 0.25 M monochromator. *trans*-Stilbene isomerization ($\Phi_{iso} = 0.52$, in hexanes[22]) was used as an external standard for the measurement of quantum yields. For temperatures below ambient, a nitrogen-cooled Oxford Instruments optical cryostat (DN 1704) and ITC temperature controller were used to maintain the sample temperature within ±0.1 K of the desired value. Quantum yields for triplet-sensitized irradiation were determined on freeze−pump−thaw degassed benzene solutions containing 0.05 M benzophenone and 0.025 M t-**1**−t-**4**. Solutions were irradiated at 366 nm to low conversions (<5%) and the yield of cis isomer compared to that for 1-phenylpropene ($\Phi_{iso} = 0.51$).[7]

Correction of Low-Temperature Fluorescence Quantum Yields. Fluorescence quantum yields will be influenced while lowering temperature owing to the change of solvent viscosity, refractive index, and volume. The application of a linear correction (eq i) was found to give corrected quantum yields consistent with fitting of our other temperature-dependent data.

$$\Phi_f = \Phi_f^{\,0} \times (A + BT) \tag{i}$$

$$A + BT_{RT} = 1 \tag{ii}$$

$$\Phi_f^{\,0} = \frac{k_f}{k_f + k_{isc} + A_{twist}\exp\left(\frac{-\Delta E_{twist}}{RT}\right) + A_{pv}\exp\left(\frac{-\Delta E_{pv}}{RT}\right)} \tag{iii}$$

In this approach, no correction is made for room-temperature measurements and the magnitude of the correction factor increases as the temperature decreases. Observed fluorescence quantum yields, Φ_f, were fit over temperature based on the above equations (i−iii), and phenyl-vinyl bridging activation parameters were obtained that are comparable to those obtained from singlet lifetime fitting. For t-**4**, phenyl-vinyl bridging activation parameters obtained by fitting the temperature-dependent fluorescence quantum yield data to eqs i−iii were similar to those obtained by fitting temperature-dependent singlet lifetime data (e.g. Figure 4: $A_{pv} = 5.6 \times 10^{10}$, $\Delta E_{pv} = 2.0$ kcal/mol). The corrected fluorescence quantum yields can be calculated using eq iii.

Data Fitting. All data fitting procedures were carried out by using either Origin (version 6)[23] or Mathematica (version 4.0).[24] The fitting strategy involved the use of as many experimental data points as possible. In all cases 15 or more data points were used to model two to four parameters. For example, four parameters, values of k_f (from Φ_f data), k_{isc}, A_{twist}, and ΔE_{twist} (from Φ_{iso} data), were employed for modeling the lifetime data, providing two parameters, A_{pv} and ΔE_{pv} (eq 5). For the final modeling, two independent data sets were analyzed using a global optimization strategy with a Multi-Start algorithm that examines literally hundreds of staring points. To simultaneously fit two sets of data, a penalty function f is constructed,

$$f(A_j,\Delta E_j) = \sum_{T_i} [\alpha(\Phi(T_i)_{nr}^{Exp} - \Phi(T_i)_{nr}^{Fit})^2 + (\Phi(T_i)_{di\pi}^{Exp} - \Phi(T_i)_{di\pi}^{Fit})^2]$$

where superscript "Exp" indicates experimental data and "Fit" indicates calculated data. α is a scaling factor used to adjust relative error. If a large error exists in the first set of data, α will be set less than 1.0 to improve fitting for the second set of data. In our data analysis, $\alpha = 1$ and parameters A_j,ΔE_j are obtained by minimizing function $f(A_j,\Delta E_j)$.

Molecular bond angles were measured based on SCF/AM1 optimized ground-state geometries by using the HyperChem (standard version, Release 5).[25]

Acknowledgment. Funding for this project was provided by NSF grants CHE-9734941 and CHE-0100596 and by Spanish DGES Grant PB97-0339. The authors thank Igor Alabugin for fruitful discussions. This work is dedicated to Howard E. Zimmerman on the occasion of his 75th birthday.

Supporting Information Available: Temperature-dependent singlet lifetimes and quantum yields of fluorescence, trans,cis isomerization, and di-π-methane rearrangement product formation for t-**1**−t-**4** (PDF). This material is available free of charge via the Internet at http://pubs.acs.org.

JA0113652

(22) Saltiel, J.; Margianari, A.; Chang, D.; Mitchener, J. C.; Megarity, E. D. *J. Am. Chem. Soc.* **1979**, *101*, 2982−2996.

(23) Microcal Software, Inc., Northampton, MA 01060; (413) 586−2013; http://www.microcal.com.

(24) Wolfram Research, Inc., Champaign, IL 61820; (217) 398−0700; http://www.wolfram.com.

(25) Hypercube, Inc., Gainesville, FL 32601; (352) 371−7744; http://www.hyper.com.